Annual Progress Report for JFY 2004

March 3, 2005

CDF Experiment

Spokespersons
Japan S. Kim (University of Tsukuba)
U.S.A. L. Ristori (INFN Pisa), Y. K. Kim (University of Chicago)

The year 2004 marked the fourth year for the Tevatron Run-II program and the CDF Run-II experiment, which officially started in March 2001. The Tevatron accelerator has been operational with 36 bunches of protons and anti-protons, respectively, at an increased center-of-mass energy of 1.96 TeV. The improvement in the accelerator performance seen in 2003 has continued in 2004. Recently a typical peak luminosity is $\mathcal{L} = 8 \times 10^{31}$ cm^{-2} s^{-1}, with a record luminosity of 11.6×10^{31} cm^{-2} s^{-1} (Figure 1(top)). The latter has surpassed the Run-IIa goal of 8.6×10^{31} cm^{-2} s^{-1}. A weekly integrated luminosity in excess of 18 pb^{-1} has also been achieved. The total integrated luminosity in the calendar year 2004 is about 350 pb^{-1}, and the Run II total is roughly 800 pb^{-1} (Figure 1(bottom)).

The upgraded CDF detector has been functioning very well with high efficiency. The integrated luminosity recorded by CDF amounts to more than 600 pb^{-1}, five times that of Run I (Figure 2). We expect to accumulate about additional 500 pb^{-1} of data in year 2005, and approaching a total integrated luminosity of 2 fb^{-1}. After that, with further improvements to the accelerator complex, such as electron cooling in the Recycler Ring, would provide an instantaneous luminosity of 2×10^{32} cm^{-2} s^{-1} and a total integrated luminosity of 5 to 9 fb^{-1} through 2009. For operations at such a high luminosity, CDF needs further upgrades of some of the detector components. They include the replacements of the central preshower detector and upgrades to the electronics and the data acquisition system. R&D efforts for the upgrades are already under way, and some of them are already complete. The Japan group has been making significant contributions.

In the remainder of this report we summarize physics results and prospects, and detector upgrade efforts, with an emphasis on contributions from the Japan group.

1 Physics Results and Prospects in Run II

We expect a data sample corresponding to an integrated luminosity of 2 fb^{-1} in the near future. This is a twenty-fold increase in the amount of data over the previous run, Run I. Also, the Tevatron beam energy has been increased to give a center-of-mass energy of 1.96 TeV.

We plan on carrying out a broad physics program, and preliminary results have already emerged from Run-II data. We describe some of them below, along with prospects with full 2 fb^{-1} of data.

1.1 Electroweak physics

Studies of single gauge boson production continue, at a new center of mass energy of 1.96 TeV. Clean signals of $W^+ \to \ell^+\nu$ and $Z^0 \to \ell^+\ell^-$ decays have been observed in Run-II data. Figure 3 shows a transverse mass distribution of the muon and missing transverse energy system for $W^\pm \to \mu^\pm\nu$ candidates, to be used for a mass measurement. The production cross sections are measured to be $\sigma(\bar{p}p \to W^\pm X) \cdot \mathcal{B}(W^\pm \to \ell^\pm\nu) = 2.64 \pm 0.01$ (stat) $\pm$ 0.09 (syst) $\pm$ 0.16 (lum) nb and $\sigma(\bar{p}p \to Z^0X) \cdot \mathcal{B}(Z^0 \to \ell^+\ell^-) = 267.0 \pm 6.3$ (stat) $\pm$ 15.2 (syst) $\pm$ 16.0 (lum) pb, respectively.

With 2 fb^{-1} of data the $W^\pm$ boson mass will be measured with a precision of about 30 MeV/c^2. Combined with top quark mass measurements, it will provide constraints on the Higgs boson mass with a relative precision of 30%. This is illustrated in Figure 4 [1].

Another area of study concerns pair production of gauge bosons. The unified electroweak theory has a non-Abelian gauge structure, resulting in self-couplings among gauge bosons such as $W^+W^-Z^0$ and $W^+W^-\gamma$ vertices. Production of W^+W^- pairs has been observed for the first time in a hadron collider. The leptonic W boson decays are used, leading to a distinctive signature of two energetic leptons and a large transverse missing energy and no extra jets. A candidate event is shown in Figure 5. The production cross section is measured to be $\bar{p}p \to W^+W^-X) = 14.6\,^{+5.8}_{-5.1}\,^{+1.8}_{-3.0} \pm 0.9$ pb [2], consistent with a theory prediction of 12.5 ± 0.9 pb.

Production of $W^\pm\gamma$ pairs is also studied. 131 (128) candidates 195 (128) candidates with photon candidates above 7 GeV/c have been observed in the $W \to e\nu$ ($\mu\nu$) channel among 200 pb^{-1} of data. Kinematic distributions such as photon transverse momentum distribution and the transverse mass of the lepton-photon-missing E_T system are examined and shown in Figure 6, which show good agreement with expectations. The production cross section is measured to be $\sigma(\bar{p}p \to W\gamma X) \cdot \mathcal{B}(W \to \ell\nu) = 19.7 \pm 1.7 \pm 2.0 \pm 1.1$ pb [3], to be compared with theory prediction of 19.3 ± 0.4 pb. N. Tanimoto (Okayama) performed the muon channel analysis. More detailed studies of self-couplings of the electroweak gauge bosons will be performed, including radiation amplitude zero in $W^\pm\gamma$ production.

1.2 Top quark properties

Since the top quark was discovered by CDF in 1995, tens of pair-produced top quark events were reconstructed and a various measurements of their properties were performed in a data sample of 110 pb^{-1}. However, most of the measurements were statistically limited, given the relatively small number of the reconstructed events. Therefore, all measurements are expected to improve with the increased amount of data in Run II.

The top analysis with Run-II data has produced results on measurements of the mass and production cross section using various decay channels. The production cross section has been measured using both lepton + jet and di-lepton channels. A candidate event in the lepton + jet channel is shown in Figure 7, where two b-jets are identified by secondary vertex tags. The jet multiplicity distribution of the b-tagged $W + n$-jet events is shown in Figure 8, where the excess over expected background in $n = 3$ and $n \geq 4$ bins is explained by the contributions from the top quark. The $t\bar{t}$ production cross section is measured to be $\sigma = 5.6\,^{+1.2}_{-1.0}$ (stat) $^{+1.0}_{-0.7}$ (syst) pb with this channel. The corresponding cross section from the di-lepton channel is $\sigma = 7.0\,^{+2.4}_{-2.1}$ (stat) $^{+1.7}_{-1.2}$ (syst) pb [4]. They both are in agreement with a next-to-leading order QCD calculation of $6.7\,^{+0.71}_{-0.88}$ pb for $m_{\rm top} = 175$ GeV$/c^2$.

The top quark mass is extracted using various techniques, both from the lepton + jet channel and the dilepton channel. K. Sato (Tsukuba) has used the lepton + jet channel and applied the looser second b-jet tagging method called "jet probability tags" in addition to the tigher "SECVTX" tags. Tagging two b-quark jets is particularly important in mass measurements, because it reduces not only the background but also the number of combinations that have to be considered in a given $t\bar{t}$ event. The reconstructed mass distribution is shown in Figure 9, and the extracted mass value is $m_{\rm top} = 177.2\,^{+4.9}_{-4.7}$ (stat) $\pm\, 6.6$ (syst) GeV$/c^2$ [5]. The most precise single measurement of the top quark mass thus far comes from the analysis of the events in the same channel using the Dynamical Likelihood Method [6]. It utilizes maximal information such as subprocess matrix elements and parton distributions. The reconstructed mass distribution is shown in Figure 10, and the extracted mass value is $m_{\rm top} = 177.8\,^{+4.5}_{-5.0}$ (stat) $\pm$ 6.2 (syst) GeV$/c^2$. K. Yorita (Waseda) performed this analysis for his Ph.D. thesis [7]. In both analyses the systematic uncertainties are dominated by our understanding of jet energy measurements. They have been studied extensively using real data and are expected to result in significant reduction in the uncertainty in the near future.

With 2 fb^{-1} of data the mass will be measured with a precision of about 3 GeV$/c^2$ [1, 8], and $t\bar{t}$ production cross section with a precision of 9%. Other production and decay properties will be also measured precisely, including $t\bar{t}$ spin correlations and $W^{\pm}$ boson helicity. Y. Takeuchi (Tsukuba) has been working on spin correlations using the dilepton channel, and expects to obtain a preliminary result soon. Single top quark production should be observed with more data, which should allow a direct measurement of the partial width $\Gamma(t \to W^{+}b)$ and a determination of CKM matrix element $|V_{tb}|$ to about 13%. Also, searches will be performed for new particles such as a charged Higgs boson through the top decay

$t \to H^+b$, and new resonant states decaying into $t\bar{t}$ pairs.

1.3 Bottom and charm physics

Traditionally CDF relied on leptons to trigger on and collect decays of B hadrons, such as $\bar{B} \to \ell^- \bar{\nu} X$ and $B \to J/\psi X \to \ell^+\ell^- X$. In Run II, CDF has introduced a device called SVT, which uses information from the silicon vertex detector at the second level of the trigger and calculates impact parameter of charged tracks with about 50 μm precision for $p_T > 2$ GeV/c. It enables us to collect decay products of long-lived particles such as B and charm hadrons.

Two-body decays of neutral B mesons to light pseudoscalars are observed (Figure 11) using this trigger. The signal peak is a mixture of four decay modes: $\overline{B}{}^0_d \to K^-\pi^+$, $\overline{B}{}^0_d \to \pi^+\pi^-$, and $\overline{B}{}^0_s \to K^+K^-$, $\overline{B}{}^0_s \to K^+\pi^-$. The composition have been determined using dE/dx information from the central drift chamber, leading to the first observation of the decay $B^0_s \to K^+K^-$. Direct CP asymmetry in the $B^0_d \to K^+\pi^-$ decay is looked for and measured to be $\mathcal{A}_{\rm CP} \equiv [\Gamma(\bar{B}^0_d \to K^-\pi^+) - \Gamma(B^0_d \to K^+\pi^-)] \,/\, [\Gamma(\bar{B}^0_d \to K^-\pi^+) + \Gamma(B^0_d \to K^+\pi^-)] = -0.04 \pm 0.08 \pm 0.01$, compatible and competitive with B factory measurements. Measuring time-dependent CP asymmjetries in $B^0_d/\overline{B}{}^0_d \to \pi^+\pi^-$ and $B^0_s/\overline{B}{}^0_s \to K^+K^-$ decay modes simultaneously would allow a clean determination of the CKM phase γ [10].

One of the primary CDF B physics goals is to observe $B^0_s\overline{B}{}^0_s$ oscillations and measure its frequency Δm_s. It should provide a determination of the Cabibbo-Kobayashi-Maskawa matrix elements $|V_{td}/V_{ts}|$ with less model-dependent way. This is a crucial test of the unitarity triangle of the CKM matrix. CDF plans to use fully reconstructed decays collected by SVT so as to allow precise determination of B^0_s meson momentum on an event-by-event basis. For a smaller value of Δm_s, the partially reconstructed semileptonic decays $\bar{B}^0_s \to \ell^-\bar{\nu} D^+_s X$ are also useful. Such signals have also been observed, which are shown in Figure 12. Extensive analysis efforts are currently under way to obtain a preliminary results (perhaps setting a limit) on B^0_s oscillations.

Lepton triggers still remain effective and useful channels for B physics. Figure 13 shows di-muon signals in Run-II data. Various resonance states, such as $J/\psi \to \mu^+\mu^-$ and $\Upsilon \to \mu^+\mu^-$, are observed cleanly. Thanks to a lowered p_T threshold on muons, J/ψ yield per recorded luminosity is a factor of two higher than in Run I. Various B-hadron signals such as $B^+ \to J/\psi K^+$, $B^0 \to J/\psi K^{*0}$, $B^0 \to J/\psi K^0_S$, $B^0_s \to J/\psi\,\phi$ and $\Lambda^0_b \to J/\psi\,\Lambda^0$ have been observed and are used to measure their masses, lifetimes and relative branching fractions. M. Aoki (Tsukuba) has been working on the B^+_c meson reconstruction, in particular the semileptonic decay $B^+_c \to \ell^+\nu J/\psi X$.

Single leptons are a good sample to collect and study semileptonic decays of B hadrons. S. Uozumi (Tsukuba) has been a major contributor in this area. The most recent effort has been to measure the lifetimes of the B^- and $\bar{B}^0$ mesons using the decays $\bar{B}\to \ell^-\bar{\nu} D^0 X$ and $\bar{B}\to \ell^-\bar{\nu} D^{*+} X$. Their signals are shown in Figure 14, as well as their decay length distributions. The lifetimes have been measured to be $\tau(B^-) = 1.653 \pm 0.029\,^{+0.033}_{-0.031}$ ps and

$\tau(\bar{B}^0) = 1.473 \pm 0.036 \pm 0.054$ ps, and their ratio to be $\tau(B^-)/\tau(\bar{B}^0) = 1.123 \pm 0.040\,^{+0.041}_{-0.039}$. An attempt to measure the B_s^0 meson lifetime is under way using the decay mode $\overline{B}_s^0 \rightarrow \ell^- \bar{\nu} D_s^+ X$.

1.4 Quantum chromodynamics

A wide variety of measurements will be performed at a new center-of-mass energy of 1.96 TeV. Also, increased statistics allow measurements in a wider range of spectra, e.g. highest E_T jets, photons and other objects, and with less statistical uncertainties. They will serve as precision tests of perturbative QCD calculations.

An example is a measurement of the production cross sections of J/ψ's. In Run I, CDF found a surprisingly high rate of direct production of J/ψ's, fifty times higher than theory [11]. The lowered muon trigger threshold has provided a reasonable acceptance down to $p_T^{J/\psi} = 0$. The production cross section is measured as a function of $p_T^{J/\psi}$. The value integrated over p_T and rapidity $|y| < 0.6$ is $240 \pm 1\,^{+35}_{-28}$ nb [12]. T. Yamashita (Okayama) has contributed to this analysis. The sample should also allow a better measurement of production polarization, which is very useful in discriminating various production mechanisms, such as gluon fragmentation and color octet models.

An investigation of decay length distributions of J/ψ's provides a discrimination of the sources of J/ψ's, namely prompt production vs. $B \rightarrow J/\psi$. The latter contribution has been determined over the nearly full kinematic range (Figure 15), and thus enabled a measurement of the (almost) total b-quark production cross section for the first time. The result is $\sigma(\bar{p}p \rightarrow bX; p_T^b > 0, |y^b| < 1.0) = 29.4 \pm 0.6 \pm 6.2$ μb [12]. This has helped understnad the long-standing puzzle of a possible excess of b-quark production rates over next-to-leading order QCD calculations.

1.5 New particle searches

Searches for the Higgs boson, supersymmetric particles and other new particles have been performed. Cross sections for the standard model Higgs boson production at the Tevatron is shown in Figure 16 (top) for various subprocesses. The largest contribution comes from the single production through gluon fusion, with the top quark in the loop. Associatied production with weak bosons $W^{\pm}H$ and Z^0H are smaller. The decay branching fractions of the Higgs boson are shown in Figure 16 (bottom). At low mass, say below 120 GeV/c^2, the decay to $b\bar{b}$ pairs is dominant, while at high mass the decays to weak boson pairs become dominant.

Thus far CDF has searched for the Higgs boson production in three different final states. The first, aimed for low mass Higgs, looked for the associated production $\bar{p}p \rightarrow WHX$, with the W boson decaying leptonically and the Higgs boson to $b\bar{b}$ pairs. The b quark jets are identified with displaced vertices. The main background coming from heavy flavor production in association with the W boson and top quark pair production. The number of events as well as di-jet mass distribution are examined for possible production of the Higgs boson. No excess is found and upper limits on the Higgs boson production is set at roughly one order of magnitude larger than the standard model predictions [13]. This is the thesis topic of Y. Ishizawa (Tsukuba).

The second analysis looks for the single production of the Higgs boson followed by its decays to W boson pairs. The channel is sensitive for high mass Higgs. The W^+W^- final state is identified with their decays to leptons, thus two energetic leptons and large missing transverse energy and nothing else. The dominant background is the electroweak W^+W^- production, which leads to the same signature. However, there exists a difference in the azimuthal angle correlations between the two processes. Again, no excess of events is observed and upper limits on Higgs production have been placed.

The third method looks for associated production of the Higgs boson with a weak boson $W^\pm$ or Z^0, where the Higgs boson decays to W^+W^- boson pair and one or both of the W boson can be off mass shell. There exist three weak bosons in the final state, where two of them have the same charge. They are required to decay leptonically, leading to a distinctive final state of isolated, same-charge lepton pairs, such as $e^+\mu^+$. No candidate event is observed in the search region and upper limits on production cross sections are placed [14]. H. Kobayashi (Tsukuba) has performed the analysis.

The results from the three analyses are summarized in Figure 17, where the obtained upper limits on cross sections are compared to standard model predictions. The limits are larger than the predictions by an order of magnitude, and an increase in the amount of data is crucial.

T. Ogawa (Waseda) has performed a search for pair production of scalar top quarks that subsequently decay, violating R-parity, into a tau lepton and a bottom quark [16]. One of the tau lepton is identified with its leptonic decay. The other tau lepton is identified with its decay into one- and three-prong hadrons. Five candidate events are found in the signal region with an expected background of 4.8 ± 0.7 events. An upper limit on the production cross section has been placed, and a lower limit on the squark mass of 134 GeV/c^2 is obtained at 95% C.L. [16], assuming the branching fraction of $\mathcal{B}(\tilde{t} \to \tau b) = 1.0$.

2 Detector Operations and Upgrades

2.1 Detector operations

The original upgrades to the CDF detector for Run II have been completed for a few years now. The involvement and contributions of the Japan group included :

- plug calorimeter (Tsukuba)
- silicon detectors SVX-II (Hiroshima, Okayama) and ISL (Tsukuba, Osaka City)

- data acquisition system : consumer server/logger (Tsukuba, Nagasaki) and online monitoring (Waseda)
- muon detector system (Waseda)
- time-of-flight counters (Tsukuba)
- silicon detectors for Run-IIb (Tsukuba, Okayama)

Now that the experiment is in a stable data-taking mode, the detector activities have mostly shifted to daily operations and monitoring.

However, there are still activities for further upgrades of the detector designed for expected increase in the Tevatron luminosity. We describe them here in the following subsections.

2.2 Consumer server/logger

M. Shimojima (Nagasaki) and H. Matsunaga (Tsukuba) have been responsible for the consumer-server/logger system, which, as part of the online data acquisition system, receives events from the level-3 trigger and sends to disk and tape storage devices as well as to online monitoring programs. In the original design of the system, the data transfer rate is 20 MB/s (or 80 events per second) and it has been achieved. However, with the recent improvements in the accelerator luminosity and the further increase anticipated in the near future, this rate would not be sufficient and an upgrade is needed. The upgrade will be implemented in several stages, and in 2004 a new software program was developed that allows recording of data in parallel. A test has been performed and it has been confirmed that a rate up to 40 MB/s can be achieved. In 2005 a new hardware will be introduced and a rate of 60 MB/s will be a goal.

2.3 Silicon vertex trigger SVT

SVT is a hardware at the second level of the trigger system and utilizes information from the silicon vertex detector (SVX-II) and selects tracks that have large impact parameters with respect to the production point, which is approximated with the position of the Tevatron beam. The device is implemented in Run II for the first time and has been operational very successfully. It has enabled CDF to collect particles originating from decays of long-lived heavy quark hadrons such as D and B mesons, and to reconstruct their decays which include only hadrons in the final state, such as $\bar{B}_s^0 \to K^+K^-$ and $\bar{B} \to D\pi$.

The device also needs to be speeded up for high luminosity. A new electronics board has been developed and installed in 2004, which resulted in a 30% reduction in trigger decision time. In 2005 the development of a new hit buffer board and new algorithms is planned, followed by further improvements to software. T. Maruyama and M. Aoki (Tsukuba) are involved in the SVT work.

2.4 Central preshower detector upgrade

The central preshower detector (CPR) is located behind the CDF solenoid (about one radiation length thick) and before the central electromagnetic calorimeter CEM. It samples electromagnetic showers at their early developmental stages, and plays important roles in identification of electrons and photons.

The original CPR detector is a slow gas chamber with relatively coarse segmentation. This detector suffers a serious occupancy problem once the Tevatron luminosity exceeds 10^{32} cm^{-2} s^{-1}. The solution is to replace it with a fast, finely-segmented device. CDF has adopted a device consisting of plastic scintillator with a wavelength shifting fiber for readout, similar to the preshower detector (PPR) for the upgraded plug calorimeter.

The detector was originally planned to be installed during a long shutdown in 2005. However, after the cancellation of the Run-IIb silicon detectors, the long shutdown was also deemed unnecessary and we have decided to installed it in summer 2004, one year earlier than originally planned. So the detector had to be installed in situ, not in the assembly hall.

Photons through the fibers will be read out with a photomultiplier tube. A total number of channels of 3072 is required, and we use multi-anode PMTs to reduce cost and space. The model Hamamatsu H8711A-10MOD (R5900-00-M16) has been chosen. This tube has 16 pixels with a pixel size of 4 mm $\times$ 4 mm. We would need 64 channels (four tubes) per CEM wedge, with a total of about 220 tubes including spares.

F. Ukegawa (Tsukuba) has been responsible for the multianode PMTs, and performed the developments, quality control and installation of the PMTs with Y. Yamada (Tsukuba). In 2002 10 prototype tubes were tested in terms of anode uniformity, pulse linearity, absolute gains, cross talk, magnetic field effects and so on. Anode uniformity of 10% is observed among different pixels within a tube. It has been decided to use a tapered base circuit so as to keep a good pulse linearity for large pulses. The design was finalized in 2002, and 30 production tubes were manufactured in late FY 2002 and tested. In JFY 2003 additional 170 tubes were produced, bringing the total number to 200. In the first half of 2004 the tests of those tubes were performed, and they were shipped to FNAL before August shutdown. The construction of other parts of the detector proceeded in parallel, and full installation of the detector was complete in November 2004, in time for the completion of the shutdown. Figure 18 shows part of the detector installed.

The detector has been tested using cosmic rays as the installation progressed, and with real data from proton-antiproton collisions since the operation of the experiment resumed. It is functioning satisfactory, and ready for physics analyses.

References

[1] "The CDF II detector, Technical design report",
CDF II Collaboration, Fermilab-Pub-96/390-E (1996).

[2] "Measurement of the W^+W^- Production Cross Section in $p\bar{p}$ Collisions at $\sqrt{s} =$ 1.96 TeV using Dileptn Events",
CDF Collaboration, D. Acosta *et al.*, submitted to Phys. Rev. Lett., arXiv:hep-ex/0501050.

[3] "Measurement of $W\gamma$ and $Z\gamma$ Production in $p\bar{p}$ Collisions at $\sqrt{s} = 1.96$ TeV",
CDF Collaboration, D. Acosta *et al.*, Phys. Rev. Lett. **94**, 041803 (2005) [arXiv:hep-ex/0410008].

[4] "Measurement of the $t\bar{t}$ Production Cross Section in $p\bar{p}$ Collisions at $\sqrt{s} = 1.96$ TeV Using Dilepton Events",
D. Acosta *et al*, Phys. Rev. Lett. **93**, 142001 (2004).

[5] "Measurement of the Top Quark Mass with the Collider Detector at Fermilab",
Koji Sato, Ph. D. thesis, University of Tsukuba, February 2005.

[6] K. Kondo, J. Phys. Soc. Jap. **57**, 4126 (1988).

[7] "Measurement of the Top Quark Mass by Dynamical Likelihood Method Using Lepton plus Jet Events in 1.96-TeV Proton-Antiproton Collisions",
K. Yorita, Ph. D. thesis, Waseda University, February 2005.

[8] "Review and preview of top physics at CDF", R. Roser, CDF Collaboration,
talk at the Thinkshop, top-quark physics for Run II, Fermilab, November 10 - 12, 1998.

[9] CDF Collaboration, D. Acosta *et al.*, Phys. Rev. D**68**, 091101 (2003).

[10] "B Physics at the Tevatron : Run II and Beyond",
K. Anikeev *et al.*, hep-ph/0201071 (2002).

[11] "J/ψ and $\psi(2S)$ Production in $p\bar{p}$ Collisions at $\sqrt{s} = 1.8$ TeV",
CDF Collaboration, F. Abe *et al.*, Phys. Rev. Lett. **79**, 572 (1997).
"Production of J/ψ from χ_c Decays in $p\bar{p}$ Collisions",
CDF Collaboration, F. Abe *et al.*, Phys. Rev. Lett. **79**, 578 (1997).

[12] "Measurement of the J/ψ meson and B-hadron Production Cross Sections in $p\bar{p}$ Collisions at $\sqrt{s} = 1960$ GeV",
CDF Collaboration, D. Acosta *et al.*, Phys. Rev. D **71**, 032001 (2005) [arXiv:hep-ex/0412071].

[13] "Search for New Particle $X \to b\bar{b}$ Production in Association with $W^{\pm}$ Bosons at $\sqrt{s} = 1.96$ TeV",
CDF Collaboration, CDF public note 7126 (2004).

[14] "Search for the Higgs Boson Using High-p_T Isolated Like-Sign Dilepton Events in 1.96-TeV Proton-Antiproton Collisions",
Hirokazu Kobayashi, Ph. D. Thesis, University of Tsukuba, February 2005.

[15] "Report of the Higgs Working Group of the Tevatron Run II SUSY/Higgs Workshop",
M. Carena, J. S. Conway, H. E. Haber, J. D. Hobbs, hep-ph/0010338 (2000).
"Results of the Tevatron Higgs Sensitivity Study",
CDF and D0 Working Groups, FERMILAB-PUB-03/320-E (2003).

[16] "Search for Scalar Top Quark Pair-Production in Scenario with Violated R-Parity in 1.96-TeV Proton-Antiproton Collisions",
Takashi Ogawa, Ph. D. thesis, Waseda University, February 2005.

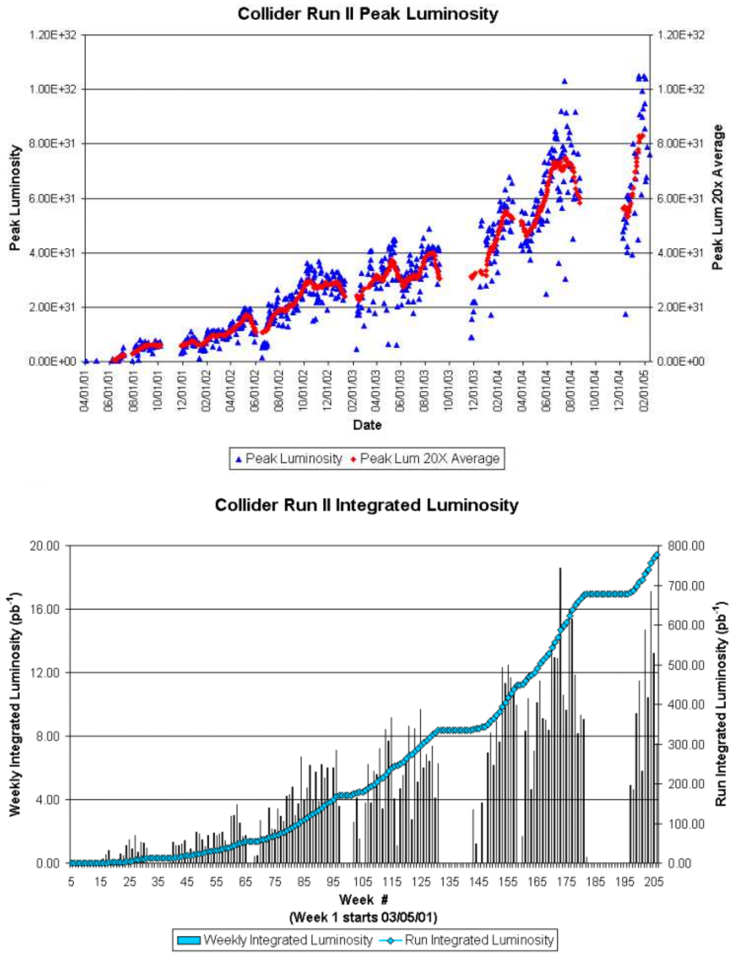

Figure 1: Tevatron performance in Run II. Top: instantaneous luminosity at the beginning of each store. Bottom: integrated luminosity delivered by week.

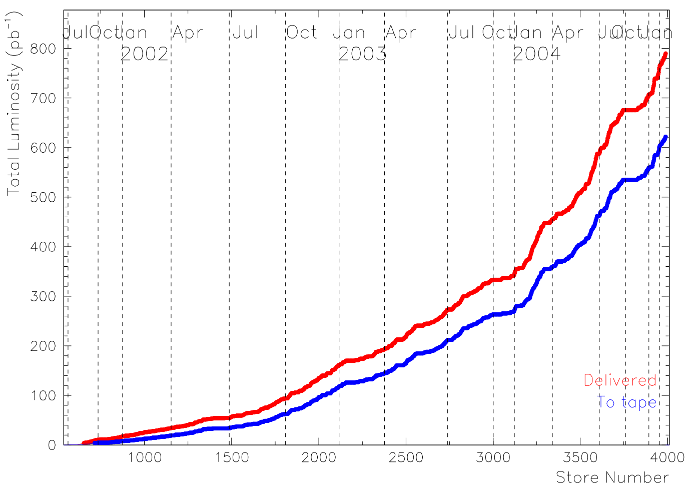

Figure 2: Integrated luminosity (top) delivered to and (bottom) recorded by CDF thus far in Tevatron Run II.

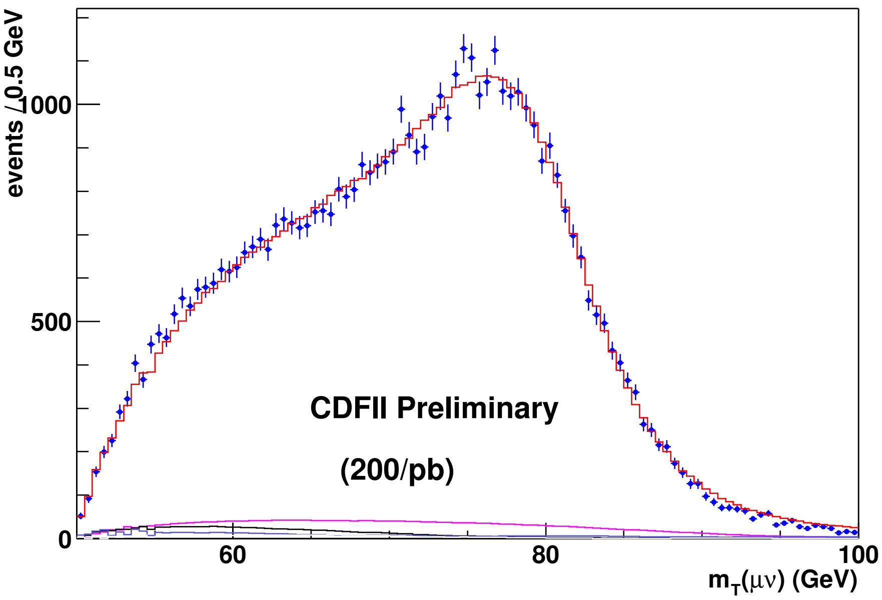

Figure 3: Transverse mass distribution of Run-II $W^{\pm} \rightarrow \mu^{\pm}\nu$ candidates.

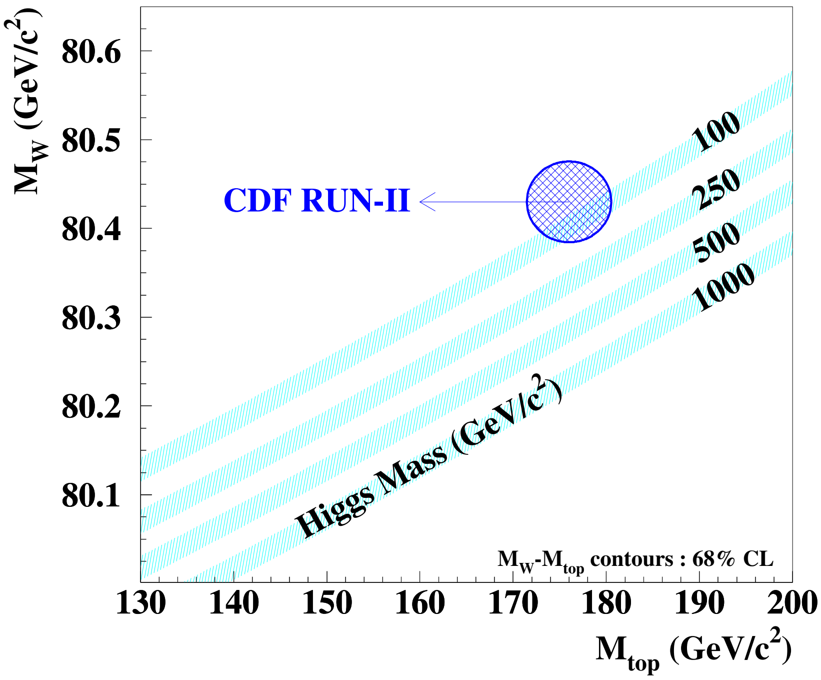

Figure 4: Expected precision in top quark and W boson mass measurements in Run II, and possible constraints on the Higgs boson mass.

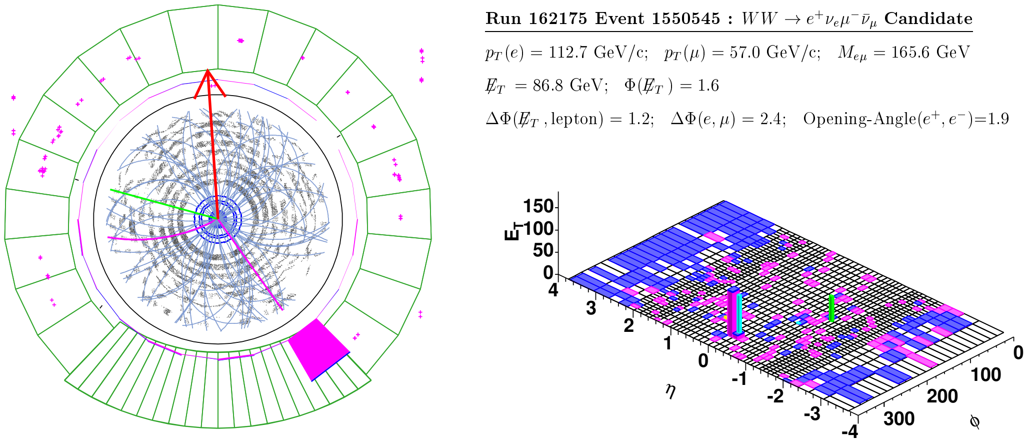

Figure 5: A display of $W^+W^- \to e\mu\nu\bar{\nu}$ candidate event.

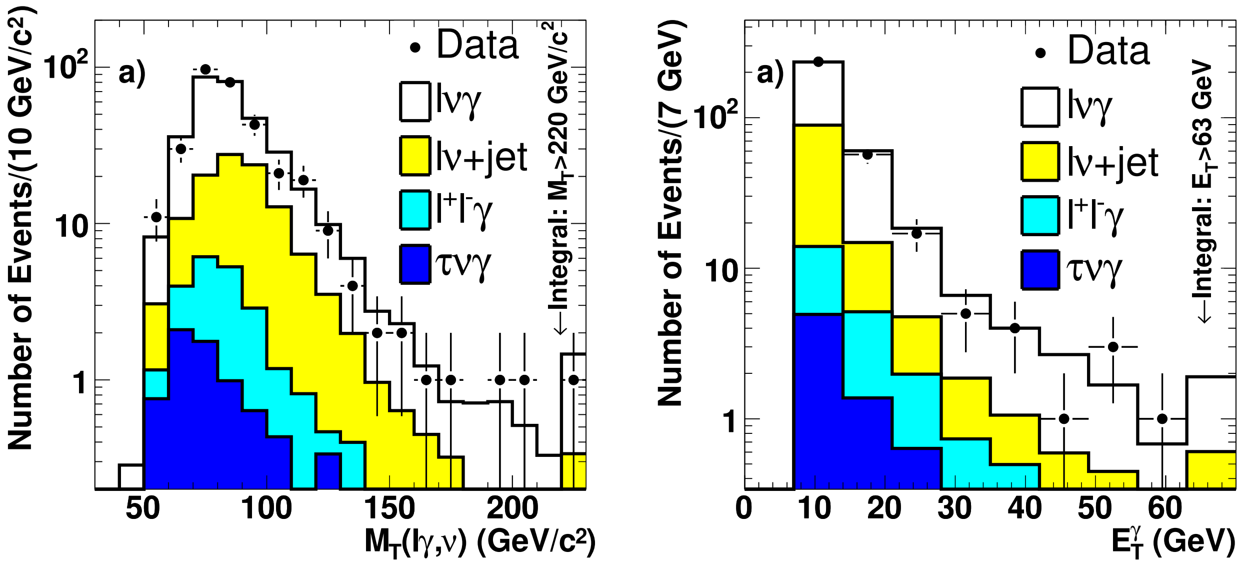

Figure 6: Transverse mass distribution of the lepton-photon-missing energy system (left), and photon transverse momentum distribution (right), in $W\gamma$ pair production candidate events.

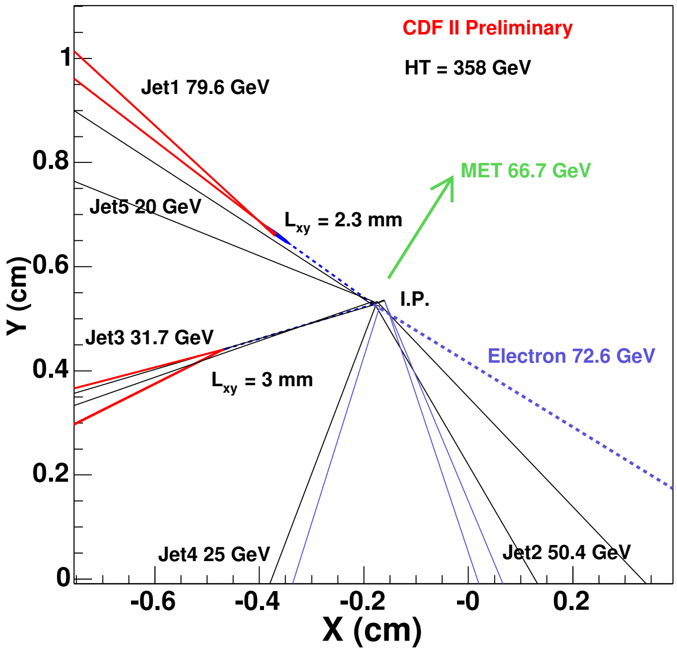

Figure 7: A top quark candidate event in the lepton + jet channel, where two b-jets are tagged by secondary vertices.

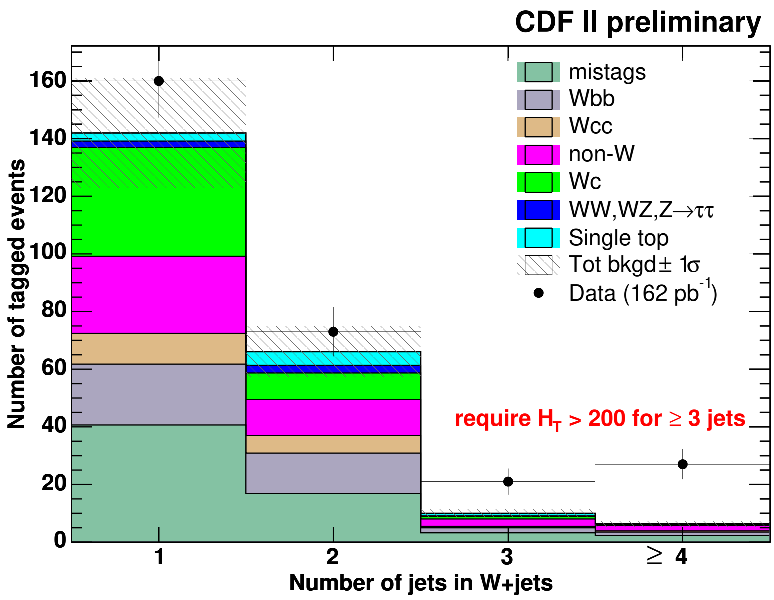

Figure 8: Multiplicity of jets in $W + n$-jet events where b-jets are tagged with secondary vertices.

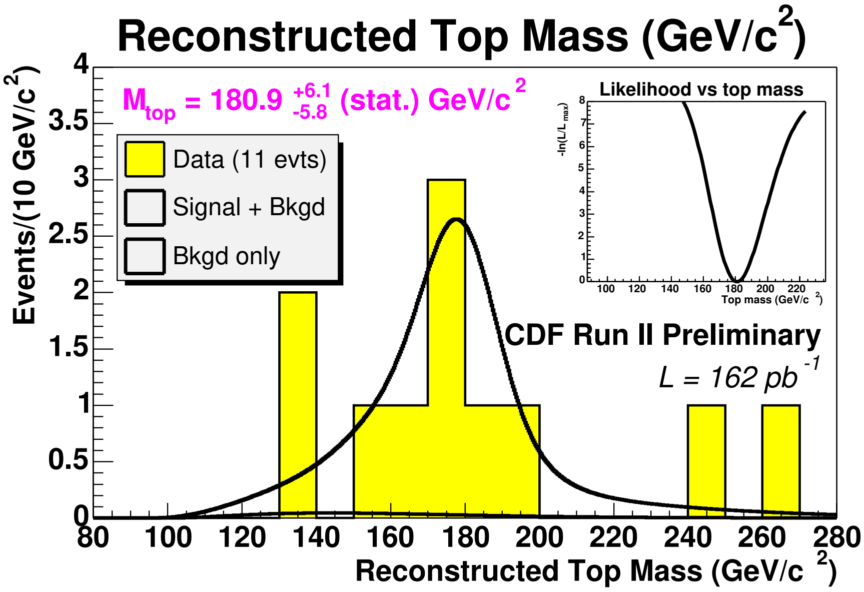

Figure 9: Top quark mass measurement from the lepton + jet channel in Run II data, with a subsample where two b-quark jets are tagged with secondary vertices.

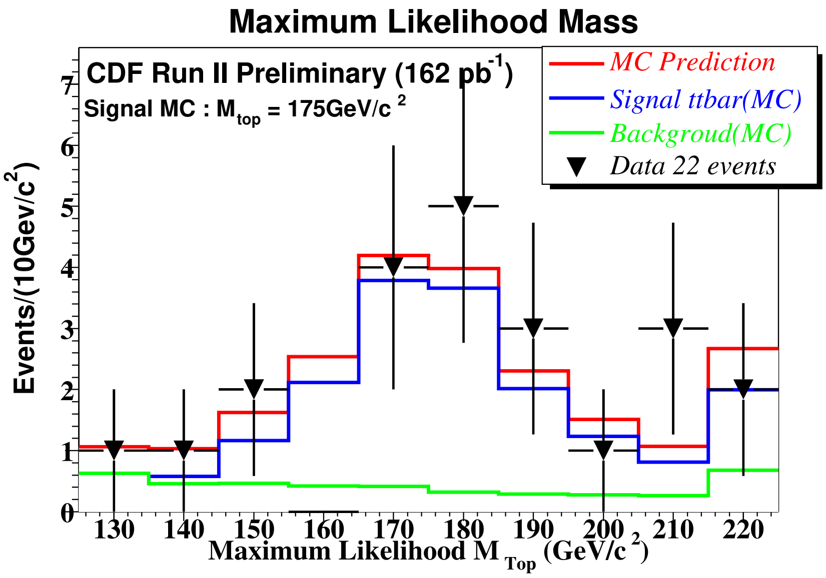

Figure 10: Top quark mass measurement from the lepton + jet channel in Run II data, using the Dynamical Likelihood Method.

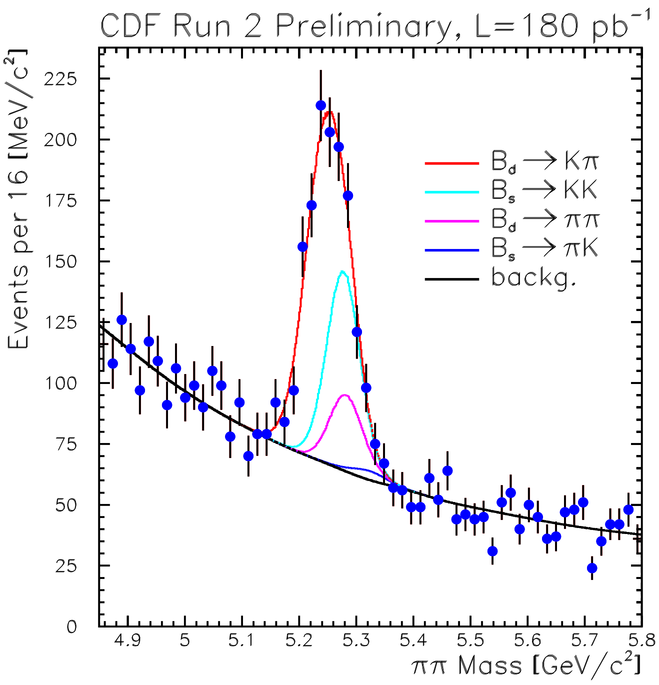

Figure 11: $B^0/B^0_s \to h^+h^-$ signal from SVT trigger, where $h^\pm$ is either $\pi^\pm$ or $K^\pm$. Pion mass is assumed for reconstruction of two-body mass. Data sample corresponds to an integrated luminosity of about 180 pb^{-1}.

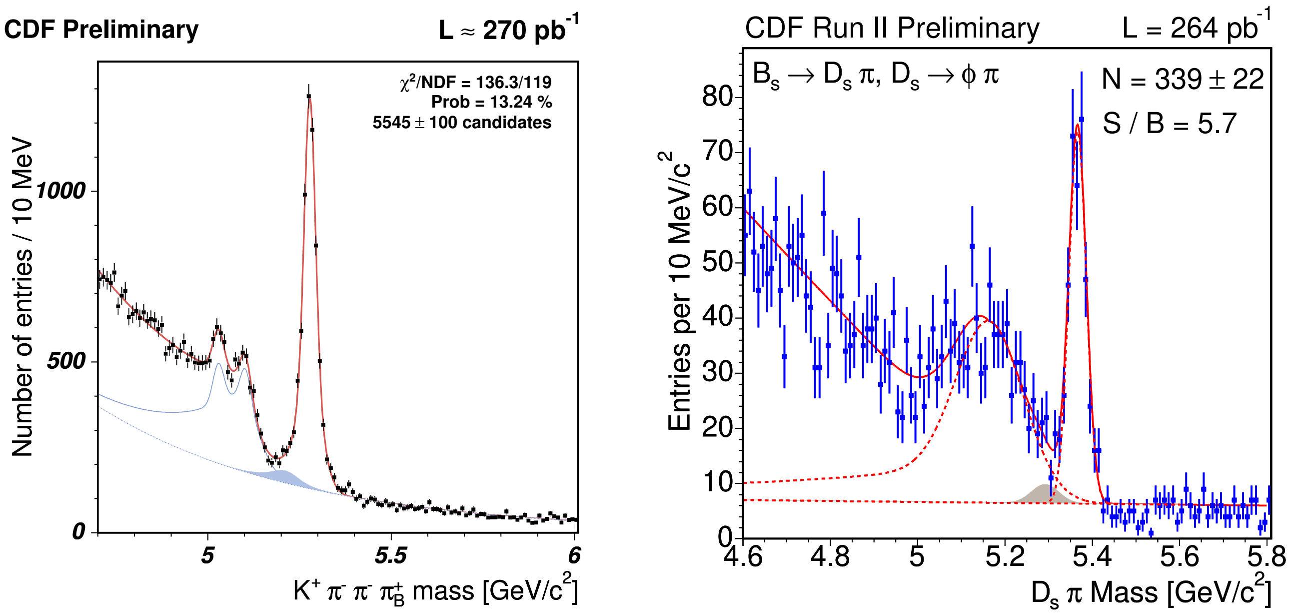

Figure 12: B meson signals from SVT trigger. Left: $\bar{B}^0 \to D^+\pi^-$, $D^+ \to K^-\pi^+\pi^+$. Right: $\bar{B}^0_s \to D^+_s\pi^-$, $D^+_s \to \phi\pi^+$.

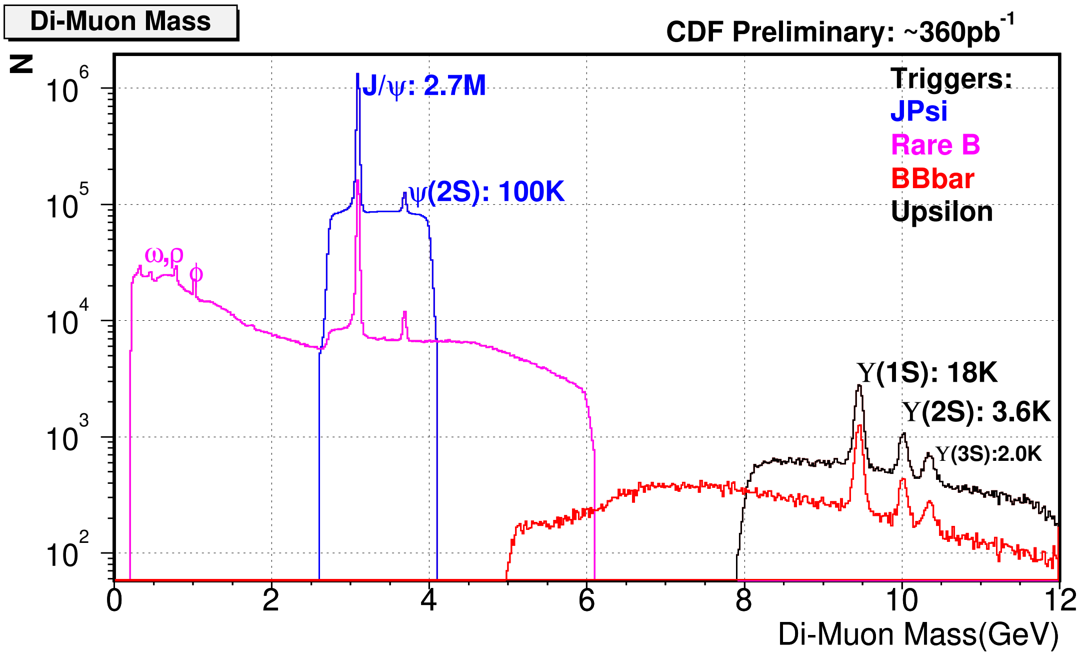

Figure 13: Invariant mass distribution of di-muon candidates. Various resonance states are seen.

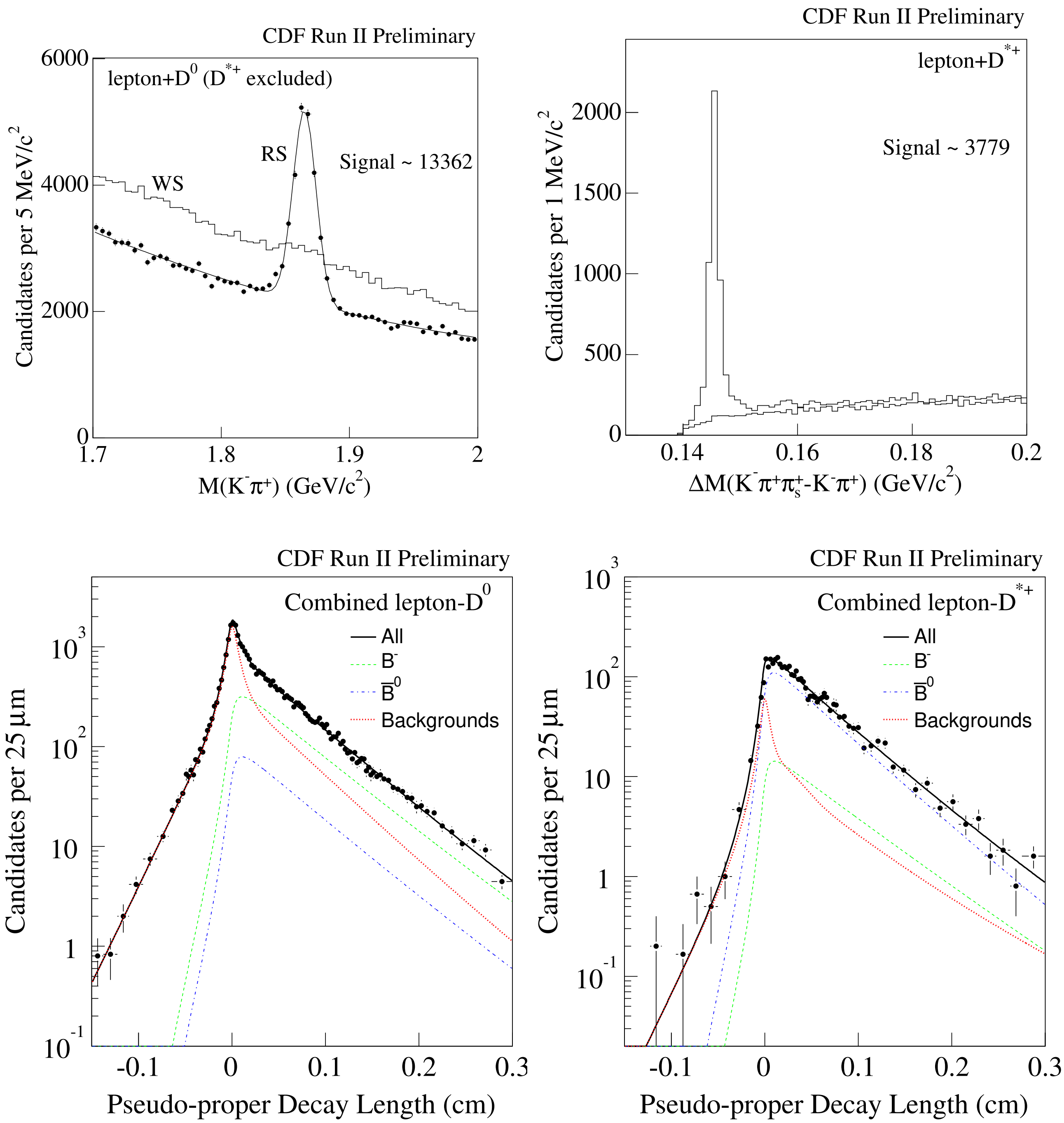

Figure 14: Top: Signals of partially reconstructed semileptonic decays of B mesons $\bar{B} \to \ell^- \bar{\nu} D^0$ and $\bar{B} \to \ell^- \bar{\nu} D^{*+}$. Bottom: Their proper decay length distributions and measurement of B^- and $\bar{B}^0$ meson lifetimes.

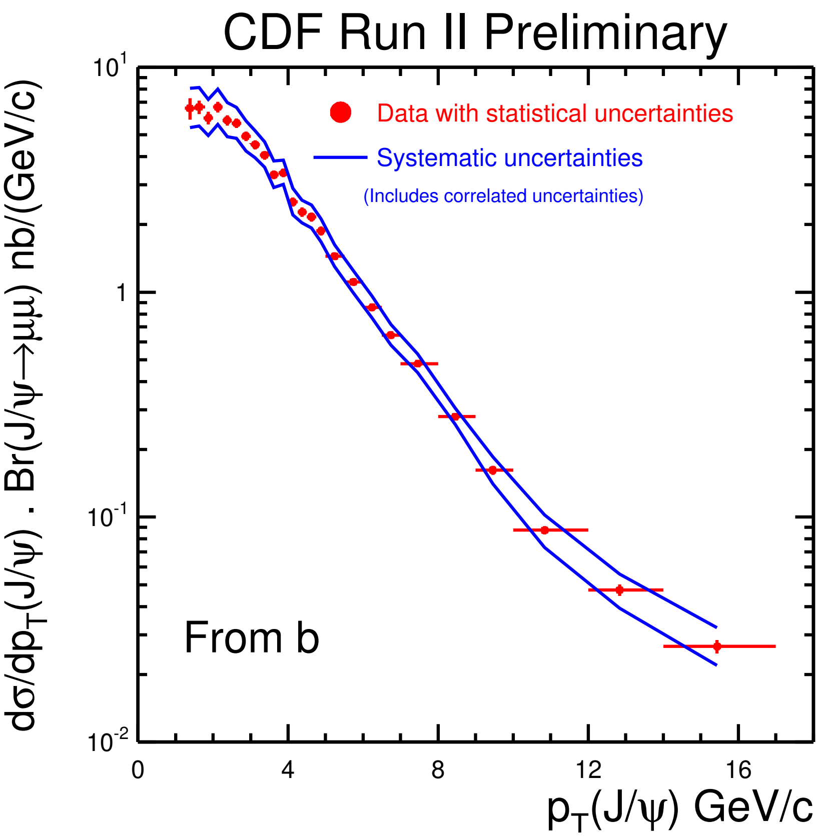

Figure 15: J/ψ production cross section from B hadrons.

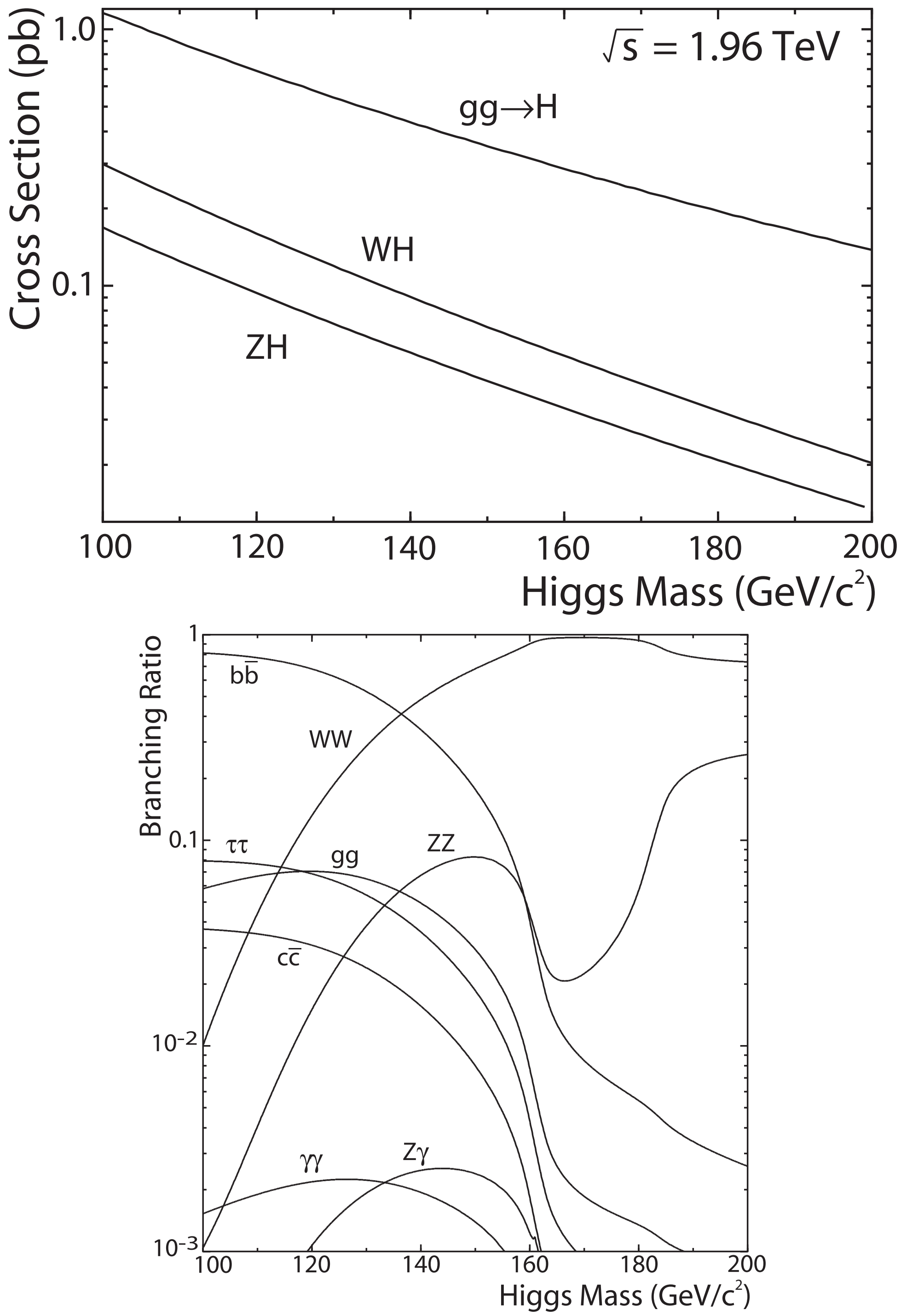

Figure 16: Top: Cross section for the production of the standard model Higgs boson at Tevatron. Bottom: Branching fractions of the standard model Higgs boson to various final states. Both plots show dependences on the Higgs boson mass.

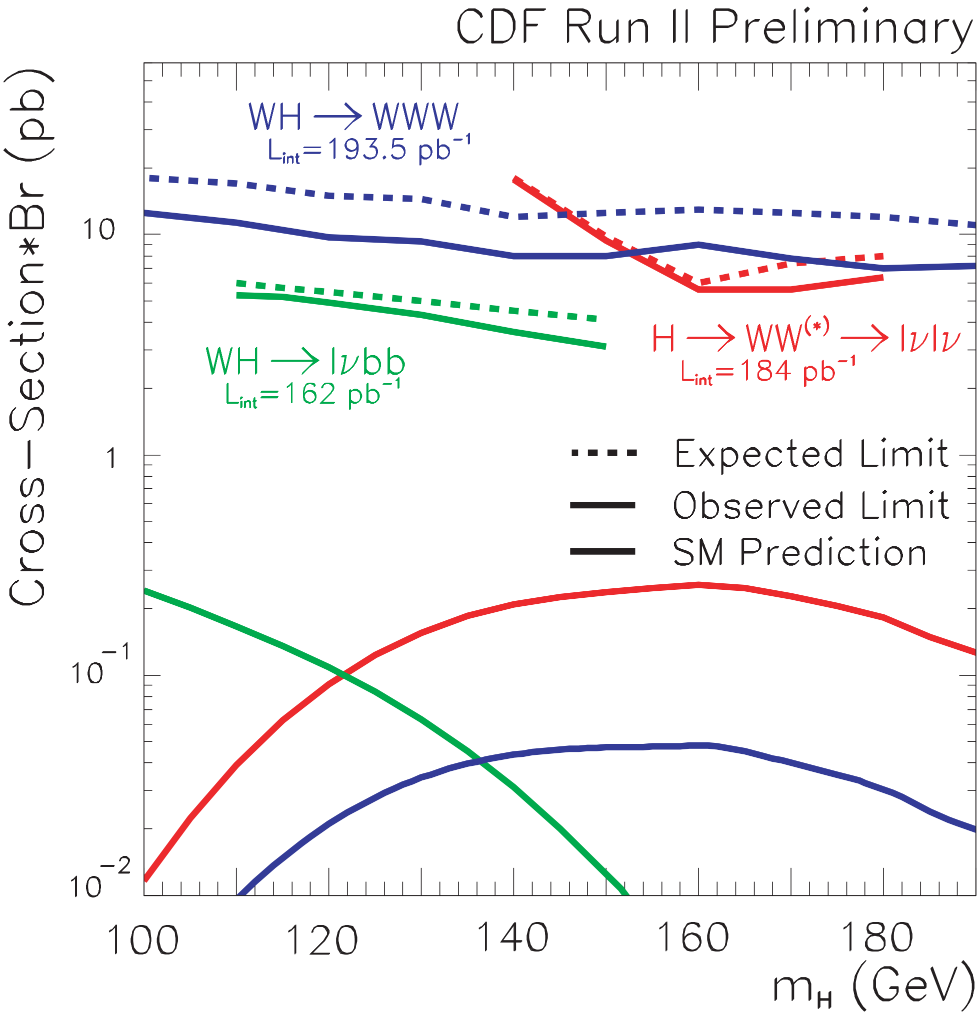

Figure 17: CDF searches for the standard model Higgs boson production in three channels. Upper limits on production cross sections are shown and compared to theoretical predictions.

Figure 18: CPR2 detector installed during summer 2004 shutdown on the face of the central calorimeter.